Cutting Dynamics Associated with Vibration
Normal to Cut Surface

By

Tetsutaro HOSHI* and Tadashi TAKEMURA*

(Received June 27, 1972)

Summary

　　Investigation into the dynamics of the metal cutting process has been carried out using a new experimental method to identify the cutting stiffness without directly measuring the dynamic cutting force.　Comparing obtained data to the theoretical formula, it has been determined that the theoretical model proposed by Das and Tobias in 1967 is valid with respect to the inner modulation effect.　Effects of cutting conditions, wave length of chatter mark, and built-up edge formation on the onset of the regenerative-type self-excited chatter are also investigated.

1.　Introduction

　　In order to advance knowledge concerning the mechanism of machining chatter so that quantitative evaluation of machine tool performance becomes feasible with respect to chatter stability, it is essential to have a proven theory of cutting dynamics.

　　In this connection, cutting dynamics are defined as the transfer function between cutting force and the tool-work relative motion in a direction normal to the mean cut surface*.　Although many attempts have been made[1]~[3] at the experimental identification of this transfer function, sufficient understanding has not yet been reached.　The principal reason resides in the technical difficulties of the experimental procedure as follows:

　　1)　Suitable exciter is not always available which is powerful and rigid enough to oscillate the cutting tool resisting the cutting force.

　　2)　Accurate measurement of the dynamic cutting force working to the tool tip is difficult to achieve at high frequencies.

　　Recent reports[4]~[6] indicate that several new methods have been attempted which, by principle, do not encounter above difficulties.

---

* Department of Precision Mechanics

* Note:　Preliminary test shows that the tool-work relative oscillation in the direction of cutting speed has negligible influence on cutting force variation as long as the frequency of oscillation is less than 1000 Hz.

In the present study, a new method similar to one of those referred to as the "stiffness method" is developed. In this method, the tool is attached to the end of a cantilever-type structure, and is excited sinusoidally by a small electro-dynamic exciter in the modal direction of the principal resonance of the structure. The dynamic exciting force applied to the tool and the oscillation of the tool are measured simultaneously. The stiffness transfer function of the cutting process is given as the vectorial difference between the dynamic stiffness of the structure apparent in cutting and in idling.

The test procedure is of advantage over the conventional method in the following points:

1) The stiffness required to support the cutting tool is provided by the cantilever-type structure, so that the exciter with a low stiffness suffices. Also, since the tool is excited in a resonance mode of the structure, enough amplitude is obtained by using a small electrodynamic exciter, which on the other hand has a high frequency ceiling.

2) In stead of a direct measurement of the cutting force, measurement is made of the force applied to the tool by the exciter, which is readily achieved by using a conventional load cell.

The transfer function data of the cutting process as obtained by this method are processed according to the shear plane theory proposed by Das and Tobias[3], so that the validity of their theory is evaluated.

2. Theoretical model

Das-Tobias' shear plane model proposed in 1967 is based on the following three assumptions:

1) Orientation of the shear plane in orthogonal cutting is unaffected by the tool-work relative oscillation.

2) Cutting force is instantaneously proportional to the area of the shear plane.

3) Geometrical orientation of the cutting force is always at a constant inclination to the instantaneous direction of cutting.

The first two assumptions define the magnitude of the instantaneous cutting force, whereas the last assumption entails the fluctuation of the working direction of the cutting force which generates seemingly new components of force variation.

In the present analysis, however, the magnitude of the instantaneous cutting force is expressed in a rather general way. Namely, when removing metal from already-made wavy surface which is referred to as "outer modulation" with a
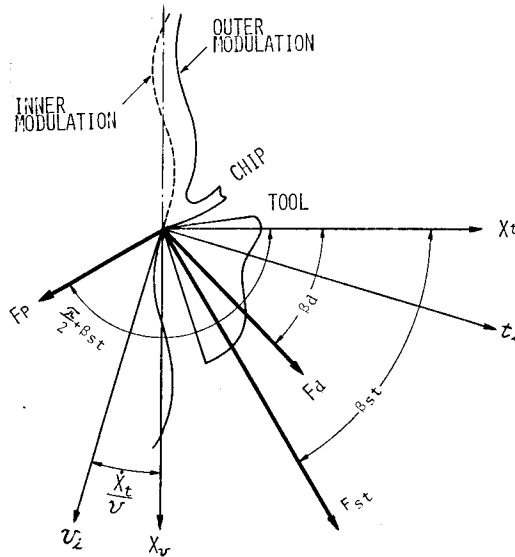
Fig. 1. Theoretical analysis of inner modulation effect.

stationary tool, the associated cutting force is expressed by combination of the static component F_{st}, and the dynamic component F_d. Geometrical orientations of those two force components are respectively represented by angles β_{st} and β_d as shown in Fig. 1.

Now, when oscillatory motion of the cutting tool itself, termed as "inner modulation", is superimposed on above situation, static component of cutting force F_{st} is intact, but dynamic component F_d will reflect the amount of metal removal affected by both outer and inner modulations. Also considering the third assumption of Das and Tobias at this stage, the working directions of the two force components F_{st} and F_d will deviate from their mean orientations by the angle $\dot{X}_t/v$ together with the t_i-v_i coordinates fixed to the instantaneous direction of cutting. Thus, resultant magnitudes of t- and v-directional components of the cutting force are formulated as follows:

$$t\text{-component} = F_{st} \cos\left(\beta_{st} + \frac{\dot{X}_t}{v} \right) + F_d \cos\left(\beta_d + \frac{\dot{X}_t}{v} \right)$$

$$v\text{-component} = F_{st} \sin\left(\beta_{st} + \frac{\dot{X}_t}{v} \right) + F_d \sin\left(\beta_d + \frac{\dot{X}_t}{v} \right)$$

Assuming cases where the angle $\dot{X}_t/v$ is small and less than the relief angle α of the tool such that the finished surface undulation does not interfere with the tool flank, and also the magnitude of F_d is far less than that of F_{st}, the above set of equations are approximated as follows:

$$t\text{-component} \simeq F_{st} \cos \beta_{st} - \frac{\dot{X}_t}{v} F_{st} \sin \beta_{st} + F_d \cos \beta_d$$

$$v\text{-component} \simeq F_{st} \sin \beta_{st} + \frac{\dot{X}_t}{v} F_{st} \cos \beta_{st} + F_d \sin \beta_d$$

$$(1)$$

The first and the third terms of the right-hand side of eq. (1) are identical to the original static and dynamic components, F_{st} and F_d, respectively, whereas the second terms represent a seemingly new dynamic force associated with the inner modulation. Denoting this new force variation by F_p, it is known from eq. (1) that

$$F_p = \frac{\dot{X}_t}{v} F_{st} \tag{2}$$

and that, F_p is in quadrature phase with the inner modulation X_t. Therefore, F_p is hereafter referred to as the "imaginary part of the inner modulation effect". Geometrical orientation of F_p is known from eq. (1) to be perpendicular to F_{st} as indicated in Fig. 1.

Eliminating the first static term F_{st} from eq. (1), the dynamic cutting force consequently consists of the force variations F_d and F_p, working at the angles β_d and $\pi/2 + \beta_{st}$ respectively from the t-direction.

In preparation for the above theoretical consequence with the experimental data at later stage, three force components F_{st}, F_d, and F_p are expressed using specific cutting forces as follows:

    (1)   Static cutting force F_{st}.

$$F_{st} = K_{st} s d \tag{3}$$

, where s and d denote feed and depth of cut in conventional cutting respectively or, mean chip thickness and width of cut in orthogonal cutting.

K_{st} is identical to what is generally referred to as specific cutting force in traditional cutting theory. In the present analysis, however, K_{st} is termed as "statical specific cutting force" in order to indicate contrast to its dynamical counterpart.

    (2)   Cutting force variatiation F_d reflects the variation in amount of metal removal affected by both outer and inner modulations. If we take the simplest model of the regenerative effect that it is proportional to the instantaneous chip thickness, F_d is expressed by the following equation.

$$F_d = K_d b_e (\mu e^{-j\varepsilon} - 1) X_t \tag{4}$$

In the equation (4), K_d denotes the "dynamical specific cutting force", b_e, effective width of cut as shown in Fig. 2 (equivalent to the width of cut in orthogonal cutting), and μ, overlap factor representing the ratio of the part shared by the previous finish to total length of b_e. ε is the phase lag of the outer modulation to the inner modulation, and it is calculated by first computing the fractional
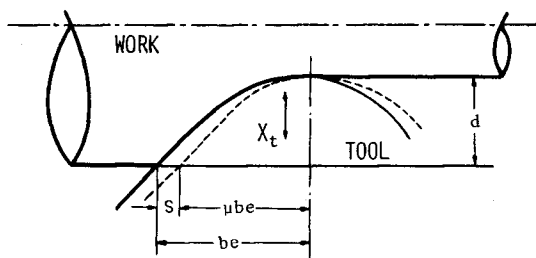
Fig. 2. Illustration of equivalent width of cut b_e in conventional turning.

part J_f of the number of undulations J per work revolution based on the frequency f of the vibration and rotational speed N of the work by:

$$J = f/N = J_i \text{ (integer)} + J_f \text{ (fraction)} \tag{5}$$

and then by:

$$\varepsilon = 2\pi J_f \tag{6}$$

On the right-hand side of eq. (4), the first term $K_d b_e \mu e^{-j\varepsilon} X_t$ reflects the variation in amount of metal removal due to the outer modulation, and the second term $-K_d b_e X_t$, that due to the inner modulation. Instead of the simplest model taken in the above, if we take the assumptions 1) and 2) of Das and Tobias' shear plane theory in defining the magnitude of force variation F_d, eq. (4) is still valid only by redefining the phase lag ε using the following equation.

$$\varepsilon = 2\pi J_f - 2\pi \frac{h_{st}}{\lambda} \cot \varphi_{st} \tag{7}$$

In eq. (7), h_{st} represents mean chip thickness, λ, wave length of the undulation, and φ_{st}, mean shear plane angle. The second term of the equation denotes the phase lag of the inner modulation to the end point of the shear plane on the outer modulation.

(3) Cutting force variation F_p, which is the imaginary part of the inner modulation effect, is written by eqs. (2) and (3) as

$$F_p = \frac{\dot{X}_t}{v} K_{st} s d$$

By assuming that the inner modulation X_t is a sinusoidal wave of a frequency f, and so writing

$$\frac{\dot{X}_t}{v} = j 2\pi f \frac{X_t}{v} = j \frac{2\pi X_t}{\lambda} \tag{8}$$

, F_p is expressed as follows:

$$F_p = j 2\pi K_{st} \frac{sd}{\lambda} X_t \tag{9}$$

Since the geometrical orientations of the dynamic forces F_d and F_p are different from each other as seen in Fig. 1, the total dynamic cutting force $F = F_d +$

F_p should be computed by taking summations of t- and v-directional components of the two forces separately. Dividing the resultant force components F_t and F_v by the tool displacement X_t, the stiffness transfer function of the cutting process is finally expressed by the following sets of equations.

$$
\left.
\begin{aligned}
T_{ct}\left(=\frac{F_t}{X_t}\right) &= T_{dt} + T_{pt} \\
T_{dt} &= K_{dt}b_e(\mu e^{-j\varepsilon} - 1) \\
T_{pt} &= -j\,2\pi K_{stv}\frac{sd}{\lambda}
\end{aligned}
\right\}
\tag{10}
$$

$$
\left.
\begin{aligned}
T_{cv}\left(=\frac{F_v}{X_t}\right) &= T_{dv} + T_{pv} \\
T_{dv} &= K_{dv}b_e(\mu e^{-j\varepsilon} - 1) \\
T_{pv} &= j\,2\pi K_{stt}\frac{sd}{\lambda}
\end{aligned}
\right\}
\tag{11}
$$

Harmonic response locus of eq. (10), for instance, is composed of a circle representing the T_{dt} term and a vertical shift of the circle due to the T_{pt} term. As shown in Fig. 3, the circle has a radius of $\mu K_{dt} \cdot b_e$, and has its center located at the point $(-K_{dt} \cdot b_e,\ 0)$ before the vertical shift. Then, the circle should be shifted downward by a distance $2\pi K_{stv}sd/\lambda$ due to the negative imaginary part of the inner modulation effect. Graphical presentation of eq. (11) is similarly conceived; but in this case, the circle is shifted upward due to the positive imaginary part.
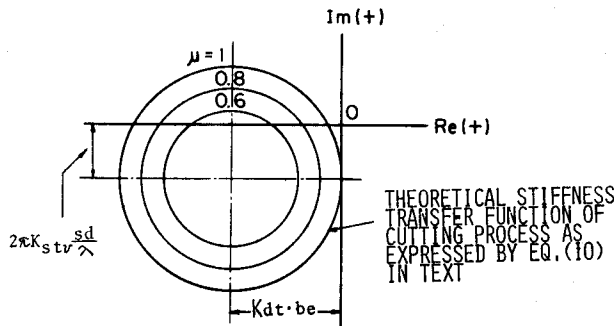

Fig. 3. Theoretical Stiffness loci of cutting dynamics in regenerative cutting.

3. Measurement of metal cutting transfer function by cutting experiments

3.1 Principle of experiments

Cutting is performed by a tool mounted on an end of a cantilever-type structure having a directional flexibility. The cutting tool is sinusoidally excited at an arbitrary frequency within the resonance frequency range of the tool support-
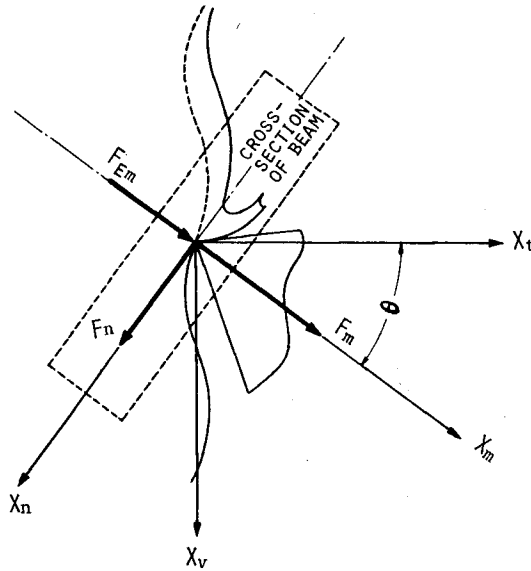
Fig. 4. Principle of experimental measurement of cutting dynamics.

ing structure. The exciting force whose instantaneous magnitude is denoted by F_{Em}, is applied in the modal direction of the tool supporting structure. Representing the modal direction by m, its normal direction by n as shown in Fig. 4, the dynamic stiffness of the structure in the two directions by T_{Mm} and T_{Mn} respectively, it is understood that T_{Mn} is far greater than T_{Mm} at the frequency range concerned, such that the motion of the cutting tool is, in matter of fact, confined to the modal direction.

Further, denoting the cutting force variation in m and n directions by F_m and F_n respectively, and the corresponding transfer functions of the cutting process by T_{cm} and T_{cn} respectively, the force equilibrium in the m-direction is formulated as follows:

$$F_{Em} + F_m = T_{Mm} \cdot X_m,$$

while F_m is expressed by

$$F_m = T_{cm} \cdot X_m.$$

The last two equations immediately produce the following formula.

$$T_{cm}\left(= \frac{F_m}{X_m} \right) = T_{Mm} - \frac{F_{Em}}{X_m} \qquad (12)$$

Similarly for the n-direction, it holds that

$$F_n = T_{Mn} \cdot X_n, \text{ and } F_n = T_{cn} \cdot X_m,$$

hence,

$$T_{cn}\left(= \frac{F_n}{X_m} \right) = T_{Mn} \frac{X_n}{X_m} \qquad (13)$$

Both direct-and cross-transfer functions of the cutting process are identified, by measuring the terms which appear in the right-hand side of eqs. (12) and (13).

3.2 Experimental procedures

As illustrated in Fig. 5, a cutting tool mounted on a cantilever-type tool supporting structure is excited by a small electro-dynamic exciter, while the longitudinal feed is engaged such that outer diameter of the workpiece is turned. Cantilever beams of four different sizes were prepared, covering resonance frequencies from 146 Hz to 1167 Hz. The modal direction of each bar is adjustable by holding the bar at any desired orientation in the t-v plane.

Referring either to eq. (5) and (6) or (5) and (7), it is expected from the theory that, when taking a fixed rotational speed $N(\sec^{-1})$ of the work, an increment of the exciting frequency f by N(Hz) causes the phase lag ε to increase by 2π. Consulting eqs. (10) and (11), this means that the transfer function of the cutting process traces a full circle in a clockwise direction. Based on this consequence, eight to ten discrete excitation frequencies are selected around the resonance frequency covering a range of N(Hz). Cutting tests are carried out at each of those frequencies taking one at a time in a random sequence.

At every frequency thus specified, the following three measurements are taken sequentially, and the data are recorded as the three plotted points in a gain-
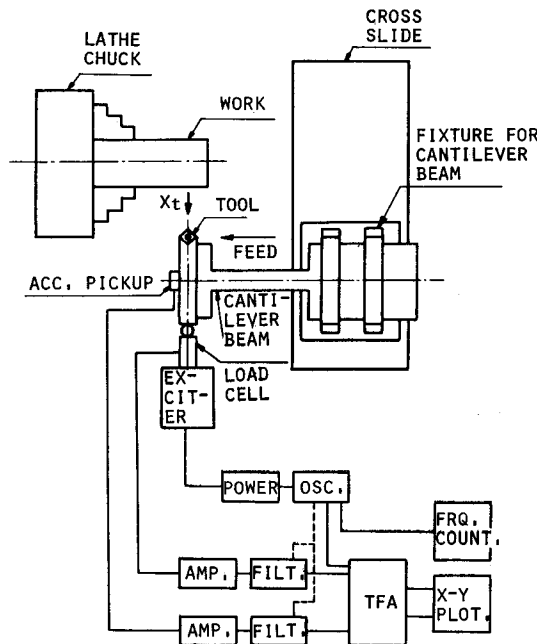

Fig. 5. Illustration of test setup.

phase graph attached on the X-Y plotter:

  i) Transfer function (T_{Mm}) between the exciting force and the vibratory displacement at idling.

  ii) Same measurement as above but at cutting (F_{Em}/X_m).

  iii) Transfer function (X_m/X_n) between vibratory displacements X_m and X_n.

Taking the vectorial difference between the first two measurements gives the direct-transfer function T_{cm} of the cutting process as indicated by eq. (12). Also multiplying the third measurement by the preliminarily measured direct stiffness of the tool supporting structure in n-direction T_{Mn}, gives the cross-transfer function T_{cn} of the cutting process as shown by eq. (13). By repeating the above process for all of the eight to ten discrete frequencies, the transfer functions are identified for a given set of cutting conditions.

In the cutting experiments, caution was taken to limit the flank wear width of the tool at 0.05 mm or less. Also the amplitude of the tool oscillation was controlled at 0.005 mm at idling, small enough to avoid interference between the tool flank and the finished surface undulation.

For the workpieces to be cut, 40 to 60 mm diameter bars of two kinds of steels were prepared whose description is as follows:

  A) P_b·S free-machining steel containing 0.08%C, 0.22%P_b, 0.31%S, and having 208 Hv hardness. This is a steel with excellent machinability.

  B) Chromium molybdenum steel for carbulization containing 0.15%C, 1.07%Cr, 0.16%M_o, specified as SCM22 steel having 200 Hv hardness. This is a steel with poor machinability.

Indexable-type turning tool with P10 carbide was used at the following tool geometries:

      side and back rake angles: $-5°$,

      side and front relief angles: 5°,

      side and front cutting edge angles: 45°,

      nose radius: 0.8 mm.

For the experimental procedures as described in the above to be correctly performed, certain conditions must be satisfied.
The conditions are:

  (1) The workpiece should not oscillate.

  (2) Linearlity should hold in the dynamic stiffnesses T_{Mm} and T_{Mn} of the tool supporting structure, as well as in the transfer functions of the cutting process, T_{cm} and T_{cn}.

  (3) T_{Mn} is far greater than T_{Mm}.

(4) Self-excited chatter should not develop when the workpiece is cut without the artificial excitation.

It was proved by preliminary tests that each of those condition is satisfied with adequate accuracies.

4. Experimental results

4.1 Typical transfer function data of the cutting process

Main parts of the experiment were carried out having the modal direction m in the direction of the depth of cut t, in which case $T_{cm} = T_{ct}$ and $T_{cn} = T_{cv}$ hold by definition.

Typical example of the measured data of T_{ct} and T_{cv} is illustrated in Fig. 6, as they are measured at eight discrete frequencies. It is immedeately seen that stiffness plots of each set fall around a circle, completing a clockwise circling for the frequency increment approximate to the work rotation speed N (3.45 Hz in the case illustrated), exactly conforming to what was anticipated from the previous theory.
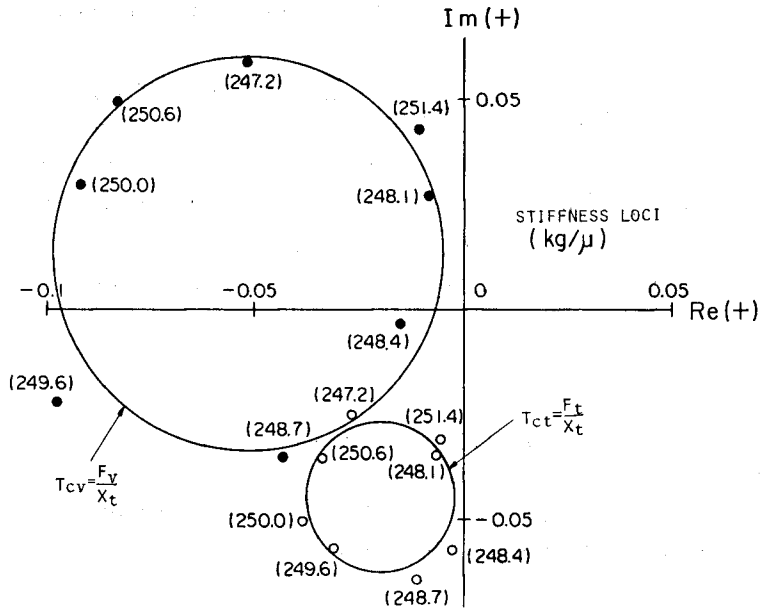

Fig. 6. Experimental results of transfer functions T_{ct} and T_{cv}. Numbers in ( ) stand for tested frequencies in H_z. Work SCM22 Steel, cutting speed 35 m/min ($v = 583$ mm/sec), depth of cut $d = 0.6$ mm, feed $s = 0.1$ mm/rev, wave length of undulation $\lambda = 2$ mm, resonance frequency of tool support 292 H_z, flank wear width $V_B = 0 \sim 0.050$ mm, work speed 207 rpm ($N = 3.45$ sec^{-1}).

The circles of T_{ct} and T_{cv} are shifted downward and upward respectively, indicating the evidence for the predicted imaginary part of the inner modulation effect represented by the T_{pt} and T_{pv} terms of eqs. (10) and (11) respectively.

Therefore, it is known that by plotting every data set as in Fig. 6, and merely by locating the centers of the circles and measuring their Re- and Im-coordinates, experimental values of the dynamical specific cutting forces K_{dt} and K_{dv} (in the form multiplied by b_e), and the imaginary parts of the inner modulation effect T_{pt} and T_{pv} are obtained.

4.2 Experimental data of dynamical specific cutting force

Dynamical specific cutting force K_{dt} in the depth of cut direction are shown in Fig. 7, 8, and 9 as measured in cutting tests at various wave lengths of undulation, cutting speeds, depths of cut, and feeds. They are illustrated by taking nondimensional ratio to the statical specific cutting force K_{stt}. Values of K_{stt} are obtained experimentally by conventional static cutting tests using a tool dynamometer, carried out at the identical cutting conditions. The statical specific
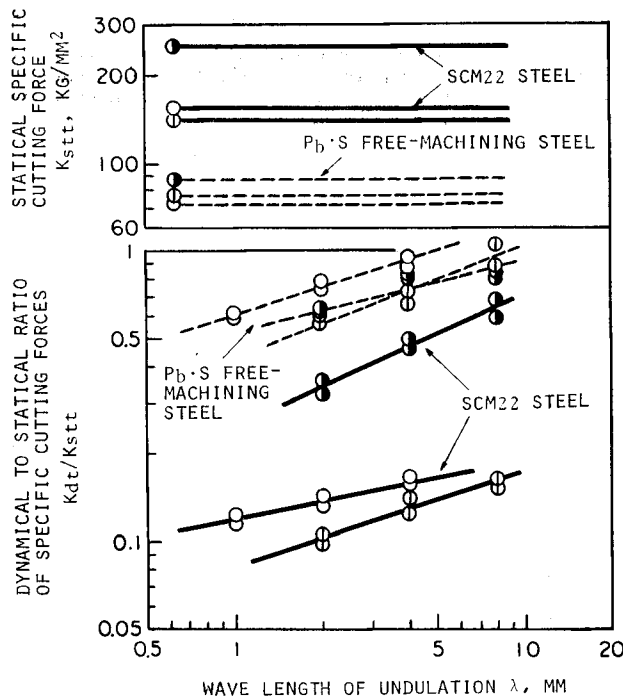

Fig. 7. Variation of dynamical specific cutting force versus wave length of undulation.

Feed $s=0.1$ mm/rev, depth of cut $d=0.3$ mm, cutting speeds $\bigcirc$ 35 m/min $(v=583$ mm/sec$)$, $\oplus$ 70 m/min $(v=1170$ mm/sec$)$, $\ominus$ 140 m/min $(v=2330$ mm/sec$)$.
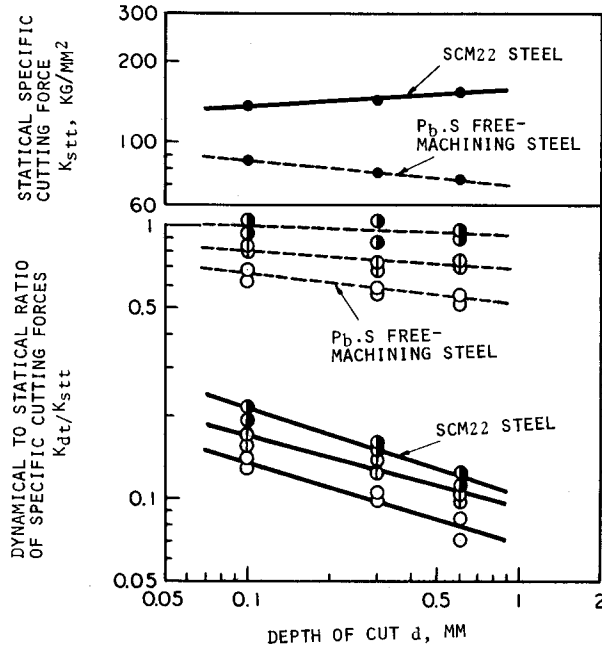
Fig. 8. Variation of dynamical specific cutting force versus depth of cut.
Cutting speed 70 m/min (v=1170 mm/sec), feed s=0.1 mm/rev, flank
wear width V_B=0~0.050 mm, wave lengths of undulation ◯ λ=2
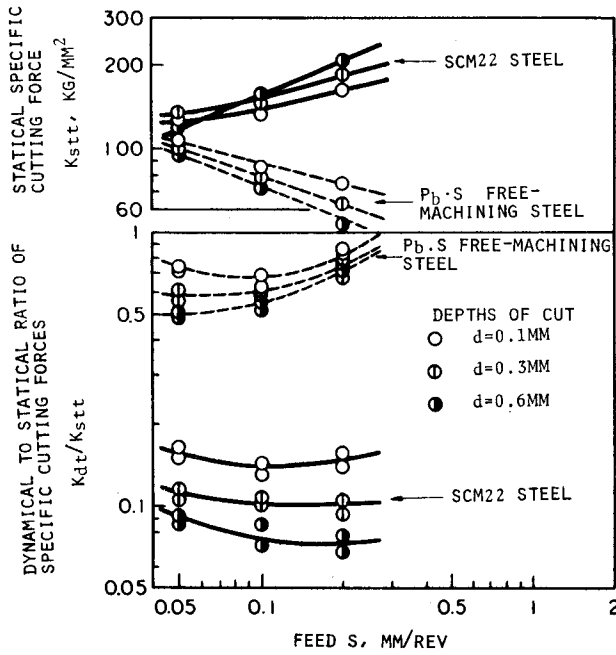mm, ◑ λ=4 mm, ◐ λ=8 mm.

Fig. 9. Variation of dynamical specific cutting force versus feed.
Cutting speed 70 m/min (v=1170 mm/sec), wave length of
undulation λ=2 mm, flank wear width V_B=0~0.050 mm.

cutting force values are illustrated for reference in the upper part of each figure.

The figures indicate that at all conditions tested, the dynamical specific cutting force is equal to or less than the statical value, and the ratio decreases as the wave length of undulation is reduced. It is noted that the ratio for SCM22 steel drastically decreases for low cutting speeds (35 and 70 m/min). Considering the observed evidence that the built-up edge was present in cutting of SCM22 steel at those low cutting speeds, the formation of the built-up edge is conceived to decrease the dynamical specific cutting force by a greater rate than it does the statical specific cutting force.

4.3 Experimental data of the imaginary part of the inner modulation effect

The imaginary part term T_{pt} was measured at various cutting conditions as listed in Table 1. Using the statical specific cutting force data K_{stv} obtained by independent static cutting tests at identical conditions, the ratio $T_{pt}/(-j2\pi K_{stv})$ was calculated and plotted in Fig. 10 versus sd/λ values, in order to check the validity of the theoretical equation (10).

It is noted that the experimental results distribute around the diagonal drawn

Table 1. List of cutting conditions for cutting tests to identify the imaginary part
of the inner modulation effect

Work steel	Flank wear width V_B	Feed s mm/rev.	Cutting speed m/min	Wave length of undulation λ, mm	Resonance frequency of tool support, H_z	Depth of cut d, mm
SCM22 steel and P$_b$·S Free-Machining steel	Kept 0.05 mm or less	0.05	70	2	583	0.1, 0.3, 0.6
		0.10	35	1	583	
				2	292	
				4	146	
			70	2	583	
				4	292	
				8	146	
			140	2	1167	
				4	583	0.1, 0.3, (0.6)
				8	292	0.1, 0.3, (0.6)
			280	8	583	0.1, (0.2), (0.3)
		0.20	70	2	583	0.1, 0.3, 0.6

Note : Depth of cut values in ( ) developed self-excited chatter when machining
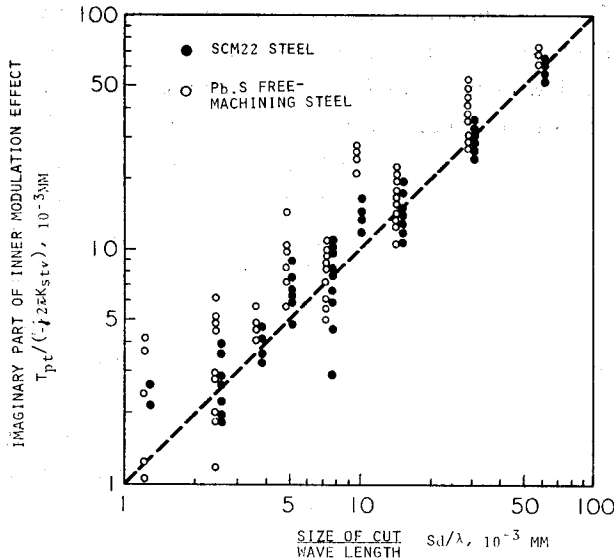SCM22 steel, thus tested for P$_b$·S free-machining steel only.

Fig. 10. Dependence of imaginary part of inner modulation effect on (size of cut)/
          (wave length) value. Broken line indicates theoretical prediction by eq.
          (10) in the text.
              s feed, d depth of cut, λ wave length of undulation. Cutting conditions
          cover whole range as listed in Table 1.

by a broken line which represents the theoretical prediction. This definitely
indicates that the theoretical model by Das and Tobias is valid with respect to
the mechanism of the inner modulation.

4.4 Geometrical orientations of the dynamic cutting forces

Geometrical orientations β_d and β_p of the dynamic cutting force components
F_d and F_p are estimated from the experimental data sets of K_{dt}, K_{dv}, and T_{pt},
T_{pv} respectively by the following computations:

$$\beta_d = \tan^{-1}\frac{K_{dv}}{K_{dt}} \tag{14}$$

$$\beta_p = \tan^{-1}\frac{T_{pv}}{T_{pt}} \tag{15}$$

From two repeated tests at the conditions identical to Fig. 6, averaged re-
sult of the orientation angles were obtained and listed in the middle column of
Table 2.

Theoretical orientation of the force variation F_p is given by $\beta_p = 90° + \beta_{st}$
according to the theory of Das and Tobias, where β_{st} is the orientation angle of
the static cutting force F_{st}. The theoretical value for this case is $\beta_p = 150°$ as
shown in the right hand side column of the Table 2 and is quite close to the ex-
perimental result of 162°.

Table 2. Geometrical orientations of dynamic cutting forces in comparison
to theoretical value

Orientations of dynamic cutting forces	Experimental Result	Theoretical value after theory of Das and Tobias
F_d	$\beta_d = 69°$	—
F_p	$\beta_p = 162°$	$\beta_p = 150°$ $(=90° + \beta_{st})$
Orientation of static cutting force	$\beta_{st} = 60°$	—
F_{st}		

(Cutting conditions are same as those for Fig. 6)

5. Interpretations of the experimental results

5.1 Low speed stability against regenerative-type self-excited chatter

Foregoing results have ascertained that the transfer functions of actual cutting process conform to the theoretical equations (10) and (11).

Considering a general case in which the modal direction m of the structural resonance is inclined to the depth of cut direction t by angle θ as shown in Fig. 4, cutting force variation in m-direction F_m is obtained from eqs. (10) and (11). Dividing F_m by the motion in the same direction $X_m = X_t/\cos\theta$ the direct stiffness transfer function of the cutting process in m-direction is obtained as follows:

$$
\left.
\begin{aligned}
T_{cm}\left(=\frac{F_m}{X_m}\right) &= T_{dm} + T_{pm} \\
T_{dm} &= K_d b_e \cos(\beta_d - \theta)\cos\theta\,(\mu e^{-j^x} - 1) \\
T_{pm} &= -j\,2\pi K_{st}\frac{sd}{\lambda}\sin(\beta_{st} - \theta)\cos\theta
\end{aligned}
\right\}
\tag{16}
$$

Harmonic response locus of this transfer function appears as one of the circles shown in Fig. 11. On the other hand, the direct stiffness transfer function of the machine structure between tool and work in its modal direction generally appears above the Re-axis as shown by an example plotted in Fig. 11. When the two loci intersect each other, it is possible for an instability to occur such that the so-called regenerative-type self-excited chatter builds up. From Fig. 11, it is understood that as far as the negative imaginary part term $-T_{pm}/j$ of eq. (16) is positive, a reduction in cutting speed, through shortening the wave length λ, shifts the stiffness circle of the cutting dynamics further downward, resulting in an increased stability.

The sign of $-T_{pm}/j$ depends on the orientation angle θ of the modal direction as follows:

$$-\frac{\pi}{2} < \theta < \beta_{st} \qquad -T_{pm}/j > 0, \qquad \text{Low speed stability,}$$
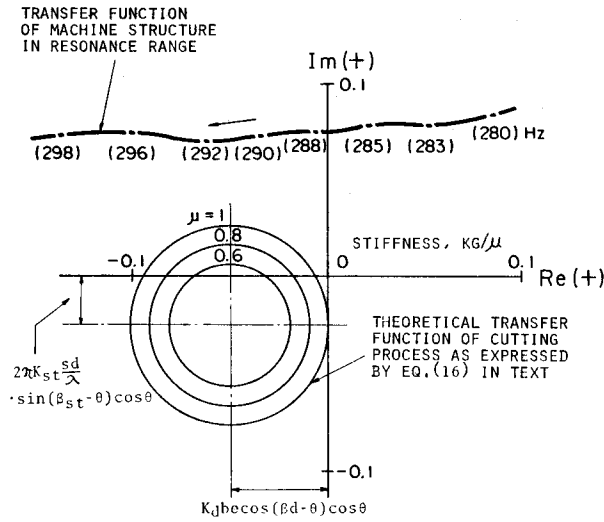
Fig. 11. Theoretical stiffness loci of cutting dynamics in regenerative cutting
when geometrical orientation of modal direction is considered.

$$\beta_{st} < \theta < \frac{\pi}{2} \qquad - T_{pm}/j < 0, \qquad \text{Low speed instability.}$$

If the orientation angle θ happens to fall within the latter range, it is anticipated
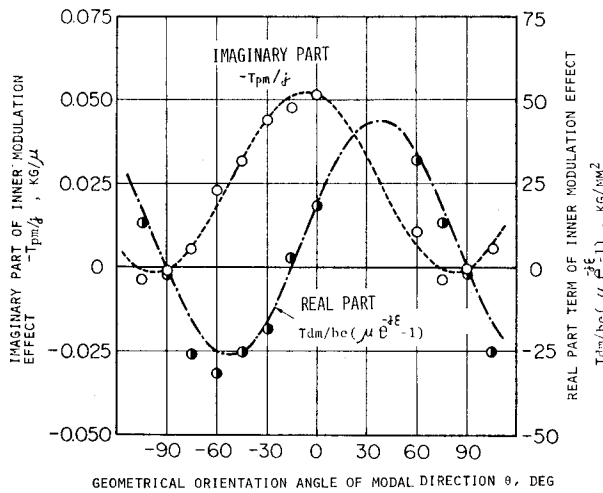that instability is more likely to occur at the lower cutting speed.

Fig. 12. Experimental data of inner modulation effect tested at various orientations
of modal direction. Curves denote theoretical predictions when assuming
$\beta_{st} = \beta_d = 75$ deg. (Work SCM22 Steel, cutting speed 35 m/min (=583 mm/
sec), depth of cut $d = 0.6$ mm, feed $s = 0.1$ mm/rev, wave length of undulation
$\lambda = 2$ mm, resonance frequency of tool support 292Hz, flank wear width $V_B =
0 \sim 0.050$ mm.)

   In order to ascertain the theoretical consequences of the above, cutting tests were performed having the cantilever tool support set at various inclination angles θ, and measuring the direct-transfer function of the cutting process in the modal direction. Experimental data of the real and imaginary parts of the center of the stiffness circle are plotted in Fig. 12. Theoretical curves of eq. (16) for $\beta_{st} = \beta_a = 75°$ are drawn in the figure. The experimental data are in good conformity to the theoretical curves, again indicating the validity of the theoretical model.

5.2 Stability against regenerative-type self-excited chatter due to formation of built-up edge

   From the results of cutting experiments comparing the two work steels, it has been perceived that the formation of the built-up edge substantially reduces the dynamical specific cutting force K_d.

   Influence of this effect on the chatter stability was demonstrated by a chatter depth experiments performed on the two work steels. The critical depths of cut at various cutting speeds obtained for the two steels are compared in Fig. 13. It is noted that the SCM22 steel shows more dominant low speed stability than
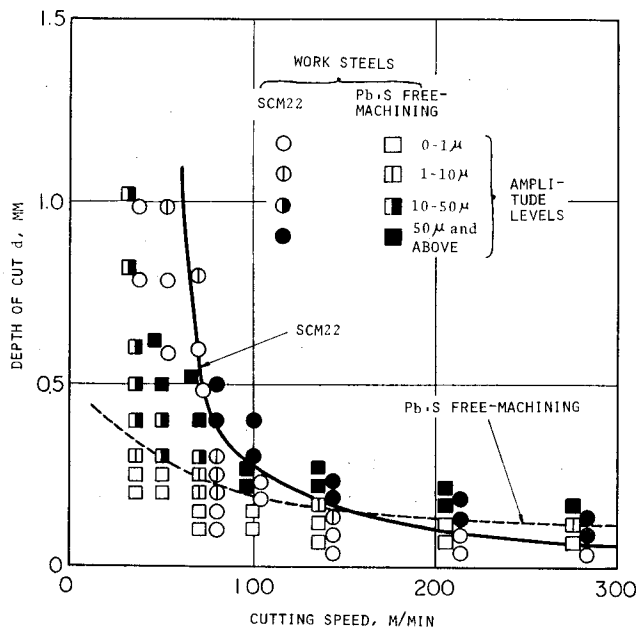

Fig. 13. Comparison of experimental curves of critical depth of cut for the two
   work steels tested.
      Feed $s = 0.1$ mm/rev, resonance frequency of tool support 265Hz, flank
   wear width $V_B = 0 \sim 0.050$ mm.
      Orientation angle of the modal direction $\theta = 0$ deg.

$P_b \cdot S$ free-machining steel. This is understood to result from the combined effect of the low speed stability due to the imaginary part of the inner modulation and the reduced dynamical specific cutting force due to the built-up edge which formed at the cutting speeds of 75 m/min and less in machining of the SCM22 steel.

6. Conclusions

A new method for measuring the transfer function between the dynamic cutting force and the tool-work relative motion was developed, and used to check the validity of the theoretical model of cutting dynamics proposed by Das and Tobias in connection with the mechanism of the inner modulation.

The following remarks are concluded from the present study:

1) Instead of directly measuring the dynamic cutting force, measurement of the exciting force applied to the cutting tool is accommodated in the new method, which, by virtue of this, can identify the transfer functions of the cutting process with adequate accuracies and in fairly simple fashion.

2) Harmonic response locus drawn by the stiffness transfer function as identified by this method is found incident to a theoretical circle, and therefore it is indicative of the validity of the regenerative effect.

3) The postulated theory involves two important parameters. One of them, dynamical specific cutting force K_d is experimentally obtained by measuring the distance between the center of the identified stiffness circle and the Im-axis. K_d values are found to be equal or less than the statical specific cutting force K_{st} measured at equivalent cutting conditions. Values of K_d depend on depth of cut, feed, and cutting speed. If those cutting parameters are fixed, K_d decreases when the wave length of undulation is reduced. K_d decreases drastically when the built-up edge is formed.

4) The other important parameter, the imaginary part of the inner modulation effect is experimentally obtained by measuring the distance between the center of the stress circle and the Re-axis. Magnitudes of the imaginary parts are found to conform to the theoretical values computed from the statical specific cutting force K_{st} by $2\pi K_{st}\, sd/\lambda$. Therefore, the theory proposed by Das and Tobias is ascertained to be valid in the inner modulation mechanism.

5) In cases where linearlity holds in the cutting dynamics, present study illustrates that the imaginary part of the inner modulation effect enhances stability at low cutting speeds when the orientation of the modal direction is properly arranged. Formation of the built-up edge also increases stability by virtue of associated reduction of the dynamical specific cutting force.

Acknowledgements

References

1) Paul Albrecht: Dynamics of the Metal Cutting Process. Winter Annual Meeting of ASME, (1964).
2) R. L. KEGG: Cutting Dynamics in Machine Tool Chatter. Trans. ASME, B, 87 (1965) 464.
3) M. K. Das and S. A. Tobias: The Relation Between The Static and the Dynamic Cutting of Metals. Int. J. Mach. Tool Des. Res. Vol. 7, (1967) p. 63–89.
4) J. Peters and P. Vanherck: Machine Tool Stability Tests and the Incremental Stiffness, Annals of the CIRP vol. 17 (1969), p. 225–232.
5) H. J. J. Kals: On the Calculation of Stability Charts on the Basis of the Damping and the Stiffness of the Cutting Process, Annals of the CIRP, vol, 19, No. 2 (May 1971) p. 297–303. H. J. J. Kals: Process Damping in Metal Cutting, Lecture to the CIRP General Assembly 1971, T. H. Eindhoven, WT-RAPPORT No. 0278, (Sept. 1971) p. 1–24.
6) J. Peters, P. Vanherck, H. Van Brussel: The Measurement of the Dynamic Cutting Coefficient, Survey Lecture to the CIRP General Assembly 1971, CRIF-MC39 (June 1971), p. 1–21.

List of symbols

α: relief angle of tool flank, deg

β_d: geometrical orientation of the force F_d, deg

β_p: geometrical orientation of the force F_p, deg

β_{st}: geometrical orientation of the force F_{st}, deg

b_e: effective width of cut, mm

d: depth of cut in conventional cutting, mm

ε: phase shift between inner and outer modulation displacements

f: frequency, H_z

F: cutting force variation $F = F_d + F_p$

F_d: cutting force variation which reflect the variation of instantaneous amount of metal removal

F_{Em}: sinusoidal force variation applied at the cutting tool by exciter in the direction of m

F_m, F_n: directional components of cutting force variation F in m- and n-directions

F_{st}: static cutting force

F_p: cutting force variation due to imaginary part of inner modulation effect

F_{pt}, F_{pv}: directional components of cutting force variation F_p in t- and v-directions

F_t, F_v: directional components of cutting force variation F in t- and v-directions

J: number of undulations per work revolution

J_f: fractional part of J

J_i: integer part of J

K_d: dynamical specific cutting force of the force variation F_d, kg/mm^2

K_{dt}, K_{dv}: directional components of K_d in t- and v-directions kg/mm^2

K_{st}: statical specific cutting force, kg/mm^2

K_{stt}, K_{stv}: directional components of K_{st} in t- and v-directions kg/mm^2

λ: wave length of the undulation, mm $\lambda = v/f$

μ: overlap factor

m: considered modal direction

n: direction perpendicular to m

N: rotational speed of work per second sec^{-1}

φ_{st}: mean shear plane angle

s: feed in conventional cutting, mm/rev

t: direction perpendicular to the mean cut surface, wherein the chip thickness is measured

t_i: direction perpendicular to v_i

T_{cm}, T_{cn}: stiffness transfer function of the cutting process in m- and n-directions, kg/mm

T_{ct}, T_{cv}: stiffness transfer functions of the cutting process in t- and v-directions, kg/mm

T_{dt}, T_{dv}: parts of T_{ct} and T_{cv} respectively due to force variation F_d, kg/mm

T_{pm}, T_{pn}: parts of T_{cm} and T_{cn} respectively due to force variation F_p, kg/mm

T_{pt}, T_{pv}: parts of T_{ct} and T_{cv} respectively due to force variation F_p, kg/mm

T_{Mm}, T_{Mn}: stiffness transfer function of the machine tool in m- and n-directions, kg/mm

θ: geometrical orientation angle between the perpendicular to the mean cut surface t and the considered modal direction m

v: cutting speed in mm/sec or index for mean cut surface direction

V_B: flank wear width, mm

v_i: instantaneous direction of cutting

X: tool-work relative oscillation in the direction given by the indices